Optical doping of waveguide materials by MeV Er implantation

A. Polman,[a] D. C. Jacobson, D. J. Eaglesham, R. C. Kistler, and J. M. Poate
AT&T Bell Laboratories, 600 Mountain Avenue, Murray Hill, New Jersey 07974

(Received 29 March 1991; accepted for publication 20 June 1991)

Implantation of MeV erbium ions into micron-thick silica and phosphosilicate glass films and 1200-Å-thick Si_3N_4 films is studied with the aim of incorporating the rare-earth dopant on an optically active site in the network. Implantation energies and fluences range from 500 keV to 3.5 MeV and 3.8×10^{15} to 9.0×10^{16} ions/cm^2. After proper thermal annealing, all implanted films show an intense and sharply peaked photoluminescence spectrum centered around $\lambda = 1.54$ μm. The fluorescence lifetime ranges from 6 to 15 ms for the silica-based glasses, depending on annealing treatment and Er concentration. Silicon nitride films show lower lifetimes, in the range <0.2–7 ms. Annealing characteristics of all materials are interpreted in terms of annealing of ion-induced network defects. These defects are identified using photoluminescence spectroscopy at 4.2 K. Concentration quenching, diffusion and precipitation behavior of Er is also studied.

I. INTRODUCTION

Optical technologies are becoming increasingly important in areas that were traditionally the domain of electronics.[1] In particular, silica-based optical waveguide fibers are now routinely used in long-distance telecommunication technology and, on a smaller scale, in local communication devices and networks. Very recently, important developments have been made on an even smaller scale, i.e., in optical integrated circuits in which planar optical waveguides on a Si substrate are employed for communication *on the wafer*. In this case, thin-film channel waveguides are used as interconnects between active devices such as lasers, amplifiers, detectors and light-emitting devices which can be processed in the Si or mounted on the wafer surface, and also in passive devices such as filters, couplers and multiplexers.[2]

Standard materials in this planar technology are silica, phosphosilicate glass, and silicon nitride. The silica-based glasses are important because they couple with low loss to standard optical fiber. The P impurity in the phosphosilicate glass raises its refractive index so that it can be used as a waveguide core in combination with a silica cladding. Single-mode waveguides are now routinely produced in this way. Silicon nitride has an even higher index, so that waveguides with smaller dimensions and tighter optical modes can be produced. Due to its index, it also couples more efficiently to semiconductor laser materials. All three of these dielectric materials are now routinely produced with high optical quality, homogeneity, purity, and stability using standard oxidation or thin-film deposition techniques[3] and a variety of planar optical devices based on these materials have been demonstrated.[4]

The newest development in optical fiber technology is the doping of the fiber core with rare-earth elements, such as Er, for use as optical fiber amplifiers and lasers.[5–8] When incorporated in a trivalent state in a solid host, these ions exhibit relatively sharp optical transitions corresponding to intra-$4f$ states. In fact, these electronic energy levels differ only slightly from those of the free ion. This is a result of the fact that the $4f$ orbitals of trivalent rare-earths are effectively shielded by the outerlying closed $5s^2$ and $5p^6$ shells. Because these transitions are in principle forbidden for electric dipole radiation by the parity selection rule, their lifetimes are relatively long.[9] Eribum is of particular interest because of its intra-$4f$ transition with a wavelength (λ) around 1.54 μm, coinciding with the low-loss window of standard optical telecommunications silica fiber.

The next challenge is to apply this optical doping technique to thin-film waveguides, in order to produce optical amplifiers or lasers on a Si substrate. These devices can then be integrated with other elements on or in the chip, so that true electro-optical integration can be achieved. To date, no suitable techniques have been reported for optical doping of thin films, apart from one report about flame-hydrolysis deposition of SiO_2:Nd.[10]

In this paper we present an investigation of optical doping of micron-thick silica, phosphosilicate, and silicon nitride films using MeV Er implantation.[11] High-energy implantation has the important advantage that the implant profile can be accurately tuned on a micron depth scale, the typical dimension of optical waveguides, and other integrated electro-optical structures. Indeed, MeV ion beams have previously been used to modify the refractive index of insulators and electro-optic crystals with the aim of producing planar optical waveguides.[12,13] Experiments have been reported in the literature on Er implantation using medium-energy ion beams. These data concern implantation into Si,[14–17] III-IV compound semiconductors,[17,18] and $LiNbO_3$.[19] In this study, we will show that optically doped waveguide materials can be successfully prepared using MeV ion implantation. Photoluminescence spectroscopy is used to study the optical properties of the incorporated rare-earth ions. Their interaction with the dielectric matrix is investigated through measurements of the lifetime of optical transitions. In addition, annealing characteristics are investigated, as well as concentration quenching effects, diffusion and precipitation behavior.

[a] Present address: FOM-Institute AMOLF, P.O. Box 41883, 1009 DB Amsterdam, The Netherlands.

 © 1991 American Institute of Physics

Downloaded 15 Sep 2003 to 131.215.237.184. Redistribution subject to AIP license or copyright, see http://ojps.aip.org/japo/japcr.jsp

II. EXPERIMENT

A. Thin-film deposition

Silica glass (amorphous SiO_2) films, 10 μm thick, were grown on Si(100) substrates by thermal oxidation in a high-pressure steam ambient. Phosphosilicate glass films were deposited using low-pressure chemical vapor deposition from silane, oxygen, and phosphine, and are referred to as P glass. Films with a thickness of 2 μm were deposited onto a Si substrate. The total P content was 7 at. %. Silicon nitride films were deposited using low-pressure chemical vapor deposition from dichlorosilane, ammonia, and oxygen. Films with a thickness of 1200 Å were deposited onto 15-μm-thick silica films on a Si substrate. The Si_3N_4 films were covered with 2000-Å Al deposited by conventional sputtering techniques. After Er implantation, the Al was removed by etching the sample in a 30 wt.% KOH/70 wt.% H_2O solution at room temperature for 3 min.

B. Ion implantation

Erbium implantation was performed using a 1.7-MV National Electrostatics Corporation 5SDH-4 tandem accelerator. The ErO^- ions were extracted in a sputter ion source from a cathode containing a mixture of Er and Al powder. The negative molecules were dissociated and charge-exchanged in a gas-stripper canal in the high-voltage terminal and the resulting Er^+ or Er^{++} ions were mass-selected in a switching magnet. All six Er isotopes were scanned through an aperture of typically 1×1 cm^2 size. The typical beam current on target was 0.5 μA. The implantation fluences ranged from 3.8×10^{15} to 9.0×10^{16} ions/cm^2 and the energies ranged from 550 keV to 3.5 MeV. All implants were performed with the samples kept at room temperature. Thermal annealing was carried out on some samples with a tube-furnace at a base pressure below 10^{-6} Torr.

C. Structural analyses

After implantation, Er concentration profiles were measured as a function of depth using Rutherford backscattering spectrometry (RBS) employing a 2.0 or 4.0-MeV He beam and a scattering angle of 170°, resulting in a depth resolution of 200 or 600 Å, respectively. Cross-sectional transmission electron microscopy (TEM) was employed to study precipitation phenomena in some samples.

D. Optical characterization

Photoluminescence (PL) measurements were performed at room temperature and at 4.2 K, the latter by immersing the samples in liquid He. The 488-nm line of an Ar^+ laser was used as a pump source and an excitation power of 250 mW was used for most PL spectra. Luminescence spectra were detected using a 0.75-m Spex monochromator and a liquid-nitrogen-cooled germanium detector. The spectral resolution ranged from 10 to 40 Å. The pump signal was mechanically chopped at 10 Hz and the signal was collected using a lock-in amplifier. Fluorescence decay measurements were performed using a 1.9-ms pump pulse with a 750-μs fall time, also obtained by mechanical chopping.

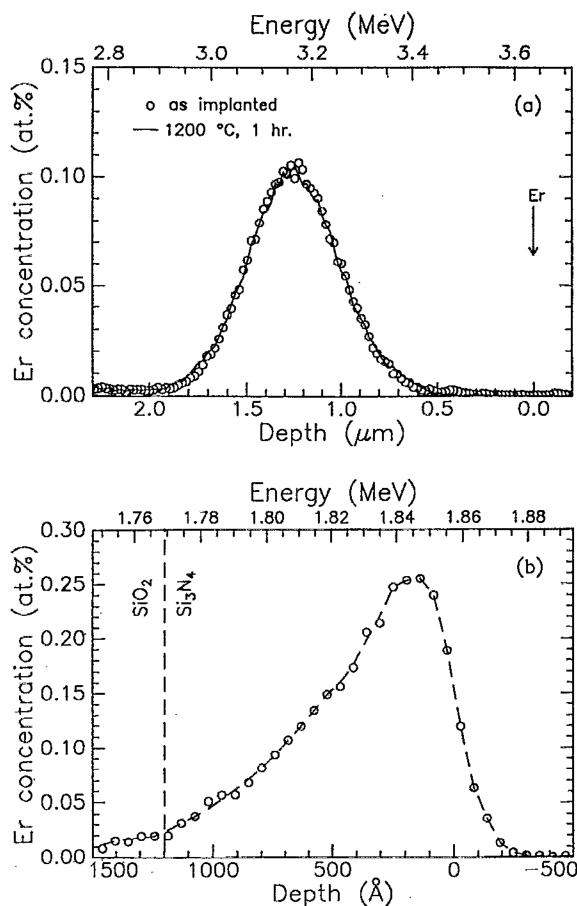

FIG. 1. RBS spectra of Er-implanted films. (a) Silica implanted with 5.0×10^{15} Er ions/cm^2 at 3.5 MeV. Spectra for as-implanted (circles) and annealed (1200 °C, 1 h, line) films are compared. (b) Al/Si_3N_4 multilayer implanted with 4.3×10^{15} Er ions/cm^2 at 550 keV, after etching off the Al surface layer. The dashed line is a guide for the eye.

III. RESULTS AND DISCUSSION

A. Implantation profiles

Figure 1(a) shows an RBS spectrum for a silica film implanted with 5×10^{15} Er ions/cm^2 at 3.5 MeV. The Gaussian-shaped Er profile peaks at a depth of 1.25 μm and has a full width at half-maximum (FWHM) of 0.56 μm. The peak Er concentration is 0.10 at.%. The figure also shows a spectrum for an implanted sample annealed at 1200 °C for 1 h. As can be seen, no noticeable diffusion of Er is detected. Similar implants into P glass also showed Gaussian-shaped Er profiles with no measurable diffusion at 1000 °C (1 h.).

Figure 1(b) shows a RBS spectrum for the $Al/Si_3N_4/SiO_2$ multilayer structure after implantation with 4.3×10^{15} Er ions/cm^2 at 550 keV. Before analysis with RBS, the Al surface layer was etched off. For this implantation energy, the Er projected range lies in the Al near the Al/Si_3N_4 interface, so that a major part of the implanted Er is removed after etching. This explains the

Downloaded 15 Sep 2003 to 131.215.237.184. Redistribution subject to AIP license or copyright, see http://ojps.aip.org/japo/japcr.jsp

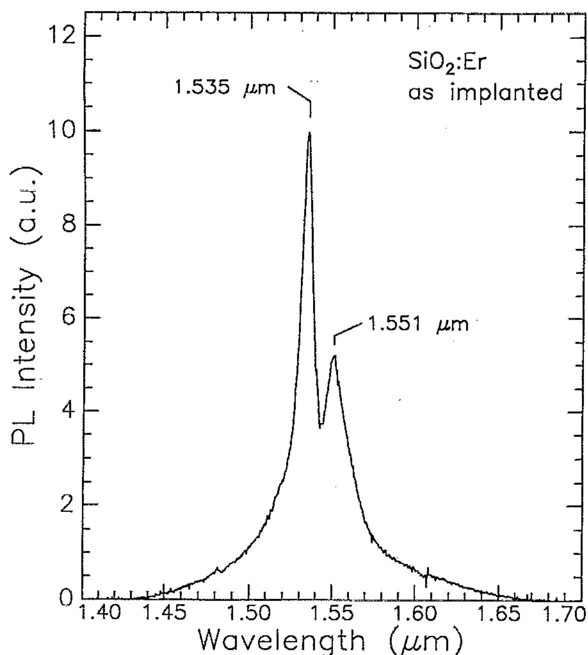

FIG. 2. Room-temperature PL spectrum for an as-implanted (5.0×10^{15} ions/cm^2, 3.5 MeV) silica film (λ_{pump} = 488 nm, spectral resolution = 10 Å).

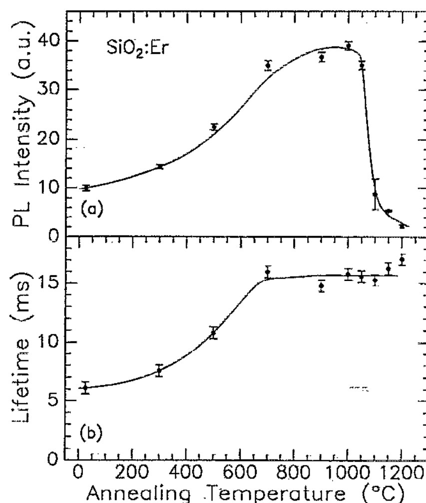

FIG. 3. (a) Room-temperature PL peak intensity and (b) fluorescence lifetime for implanted silica films measured at λ = 1.535 μm, as a function of annealing temperature. Annealing was performed in vacuum for 1 h. The lines are a guide for the eye.

asymmetry in the Er profile; it is a decreasing function of depth with a surface concentration of ~0.25 at.%. The total surface areal density of Er after etching was 1.8×10^{15} ions/cm^2. A very small fraction of the Er profile extends into the underlying silica. Annealing at 1200 °C for 1 h. did not result in a change in the Er profile.

B. Photoluminescence

1. Silica

Figure 2 shows a PL spectrum measured at room temperature of a silica film implanted with 5×10^{15} Er ions/cm^2 at 3.5 MeV. No thermal annealing has been applied to this sample. As can be seen, the spectrum is sharply peaked at λ = 1.535 μm (806 meV) and a side peak is observed at λ = 1.551 μm. The wavelength region around 1.54 μm coincides with the wavelength of the transitions between the first excited manifold $^4I_{13/2}$ and the $^4I_{15/2}$ ground manifold of Er^{3+} ($4f^{11}$) (Ref. 9). The relatively large width of the main peak (110 Å FWHM) and the wide tails of the spectrum are a result of Stark splitting of the excited and ground state in the host field plus small additional inhomogeneous and homogeneous broadening. The two peaks are the only resolved Stark structure.

It is important to note that the as-implanted sample shows a measurable PL intensity at room temperature. This should be contrasted with the results obtained for Er-implanted semiconductors in which case an annealing treatment is always necessary to obtain Er at an optically active site, and in which case luminescence is generally only observed below room temperature.[14–18] Apparently, the bonding nature of the SiO_2 network provides the environment for the Er to be incorporated in its trivalent state, even when no annealing is applied.

After implantation, some implanted silica films have been thermally annealed in the temperature range from 300 to 1200 °C for 1 h. It is important to note that annealing did not change the overall shape of the spectra. It did however lead to an increase in the PL intensity. This can be seen in Fig. 3(a), which shows the PL intensity measured at λ = 1.535 μm as a function of annealing temperature. It should be noted that the PL intensity is determined by the overlap of the Er concentration profile and a standing wave pattern of the probe light in the glass layer. No absolute quantum yields have yet been determined. The PL intensity increases with annealing temperature in the temperature range 300–900 °C. Earlier studies have shown that annealing temperatures above 400 °C are required to anneal implantation damage, such as dangling bond and vacancy complexes (e.g., E′ and B_2 centers) as well as bond angle and length distortions in the silica network.[20–23] We therefore suggest that such damage is closely related to the Er optical activity.

To study these annealing effects in more detail, measurements of the fluorescence decay time of the $^4I_{13/2} \rightarrow {}^4I_{15/2}$ transition were performed. A schematic outline of the principle of these measurements is given in Fig. 4, which shows the energy levels involved in the present PL pump configuration. The Er is pumped to a high-lying excited state, whereupon the energy rapidly decays through nonradiative processes to the $^4I_{13/2}$ state. From there the system can decay to the ground state either through an optical transition at λ = 1.54 μm or through a nonradiative process. The purely optical decay is characterized by a lifetime in the order of 10–20 ms.[9] The nonradiative process occurs on a much smaller time scale, depending on the defect structure of the material. If the Er ion interacts with defect states this term can become dominant and the overall fluorescence decay time will become

Downloaded 15 Sep 2003 to 131.215.237.184. Redistribution subject to AIP license or copyright, see http://ojps.aip.org/japo/japcr.jsp

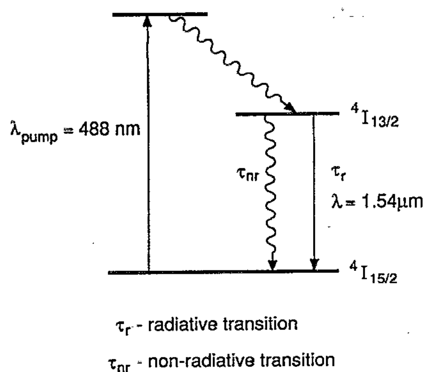

FIG. 4. Schematic of Er energy level diagram for the PL configuration.

shorter. In all fluorescence decay measurements shown from here the decay was purely exponential. It should be noted that this might be a consequence of the use of a monochromatic excitation pulse: broadband excitation might have given nonexponential decays since an ensemble of sites is excited in that case.

Figure 3(b) shows the room-temperature fluorescence decay times as a function of annealing temperature. The decay time for the as-implanted sample is 6 ms; it increases with temperature up to 700 °C, and remains fairly constant at around 15 ms for higher temperatures. First, it should be noted that the lifetime for the as-implanted sample is surprisingly high, taking into account that no thermal treatment is applied to anneal out implantation-induced defects. This shows once again that the glass network itself can accommodate these defects to a great extent as far as their interaction with the Er ions is concerned. The lifetimes reported here are an order of magnitude longer that those observed in Er-implanted Si and III-IV compound semiconductors[24] and, to our knowledge, are among the highest values reported for Er-doped glass.

The increase in lifetime in the temperature range up to 700 °C is attributed to the annealing of network defects and can partly explain the increase in PL intensity in that temperature range. To first approximation, the PL intensity should increase proportionally to the lifetime. The fact that the PL intensity increases by a factor of 4 upon annealing, while the lifetime increases by only a factor of 2.5, suggests that thermal annealing also increases the fraction of optically active Er ions.

The rapid decrease in PL intensity above 1000 °C [Fig. 3(a)] is explained by precipitation of Er, as can be seen in the cross-section TEM micrograph of Fig. 5. This micrograph is taken on a sample annealed at 1200 °C for 1 h and shows the area around the peak of the implant at 1.25-µm depth. Clearly, 100–200-Å-diam precipitates are observed. Energy-dispersive x-ray analysis revealed that these precipitates contain Er. These precipitates were not observed in samples annealed to 1050 °C. It is likely that Er ions in these precipitates do not exhibit optical transitions, hence the precipitation phenomena are not reflected in the lifetime data as these are only a probe of the optically active ions dispersed in the silica network.

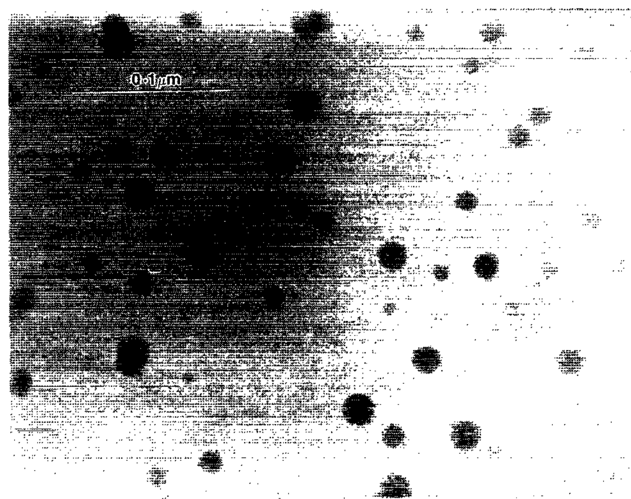

FIG. 5. Cross-section TEM micrograph of Er-implanted SiO_2 annealed at 1200 °C for 1 h. The micrograph is taken at the peak of the Er profile at ~ 1.25 µm depth.

2. P glass

Figure 6 shows room-temperature PL spectra of P glass films implanted with 3.8×10^{15} Er ions/cm^2 at 2.9 MeV. Spectra are shown for an as-implanted sample and for a sample annealed at 700 °C for 1 h. Both spectra peak at $\lambda = 1.535$ µm, while the shape of the spectra is quite different. After annealing a broad shoulder forms at the low-wavelength side and the double-peak structure disappears. This indicates a change in the local configuration of the P glass network around the Er ions upon annealing.

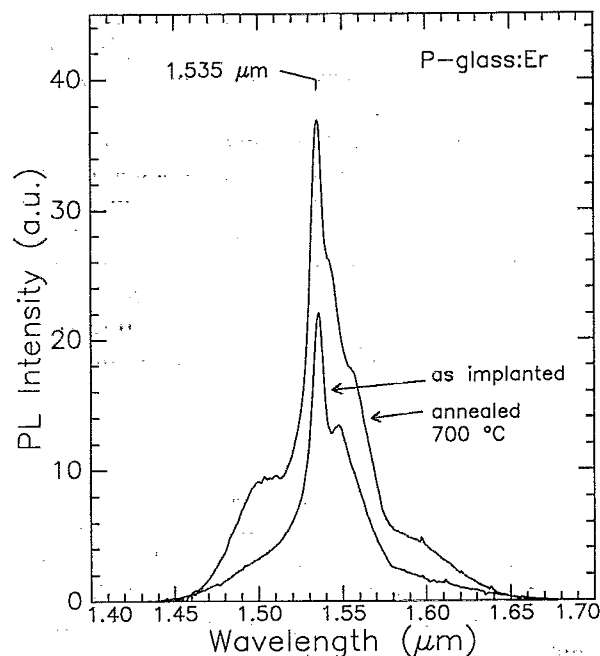

FIG. 6. Room-temperature PL spectra for as-implanted (3.8×10^{15} ions/cm^2, 2.9 MeV) and implanted + annealed (700 °C, 1 h.) P glass films. Both measurements were performed using the same pump power (λ_{pump} = 488 nm, spectral resolution = 10 Å).

Downloaded 15 Sep 2003 to 131.215.237.184. Redistribution subject to AIP license or copyright, see http://ojps.aip.org/japo/japcr.jsp

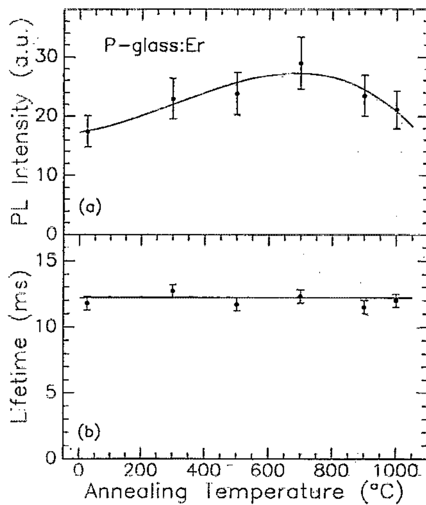

FIG. 7. (a) Room-temperature integrated PL intensity and (b) fluorescence lifetime measured at $\lambda = 1.535\ \mu$m, for implanted P glass films, as a function of annealing temperature. Annealing was performed in vacuum for 1 h. The lines are a guide for the eye.

Figure 7 represents the annealing characteristics of implanted P glass films in the temperature range 300–1000 °C. No annealing was performed for temperatures above 1000 °C, above which P glass exhibits measurable flow and above which phase separation and outdiffusion of P is known to occur. The integrated PL intensity and the lifetime measured at $\lambda = 1.535\ \mu$m are shown. A slight increase in PL intensity is observed for temperatures up to 700 °C, followed by a minor decrease for higher temperatures. The lifetime remains constant at around 12 ms over the whole range from as-implanted samples to samples annealed at a temperature of 1000 °C. These measurements show that thermal annealing does not have a large effect on the Er optical activity in P glass. In fact, the as-implanted sample shows a high lifetime (12 ms) already, and annealing does not lead to a further improvement. This indicates that the P glass network structure can accommodate the implantation-induced defects as far as their influence on optical properties is concerned. The slight increase in PL intensity upon annealing could then be explained by a small increase in active fraction; the decrease above 700 °C would then correspond to a decrease in active fraction as the temperature is approached at which structural degradation of the P glass occurs.

3. Si_3N_4

Room-temperature PL spectra of Si_3N_4 films with 1.8×10^{15} Er ions/cm^2 [Fig. 1(b)] are shown in Fig. 8 for an as-implanted and an annealed (1200 °C, 1 h) sample. The main peak is observed at $\lambda = 1.535\ \mu$m with a side peak at $\lambda = 1.550\ \mu$m. The side peak is more pronounced in the annealed sample, indicating a smaller inhomogeneous broadening component due to a more defined local geometry after annealing. There is a large difference in PL intensity between the as-implanted and annealed sample: the PL intensity increases by a factor ~ 30 upon annealing

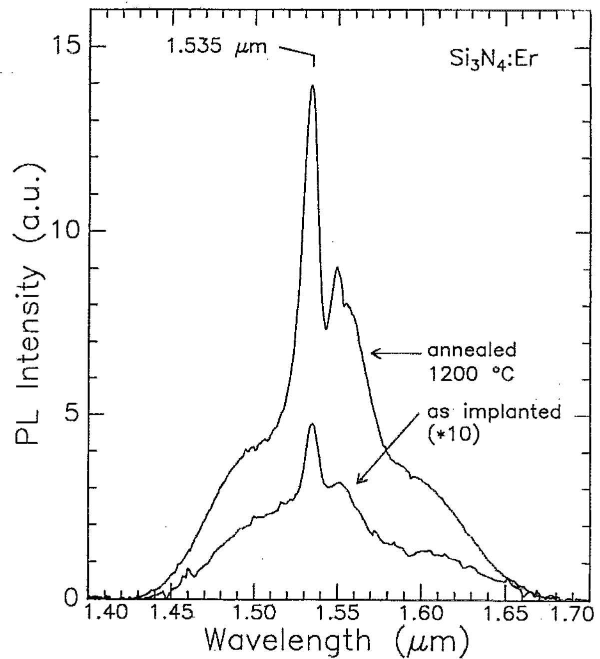

FIG. 8. Room-temperature PL spectra for as-implanted and implanted + annealed (1200 °C, 1 h.) Si_3N_4 films. Both measurements were performed using the same pump power [λ_{pump} = 488 nm, spectral resolution = 40 Å (a), 10 Å (b)].

at 1200 °C. Figure 9(a) shows the PL peak intensity as a function of annealing temperature in the range from 300 to 1200 °C. The figure shows the rapid increase of the intensity with increasing temperature and it appears that no saturation is yet observed for annealing temperatures up to 1200 °C. The lifetime as a function of annealing temperature is shown in Fig. 9(b). For annealing temperatures up to 500 °C lifetime measurements are resolution limited (resolution 230 μs). For higher temperatures an increase is observed; a maximum of 6.7 ms is found for annealing at

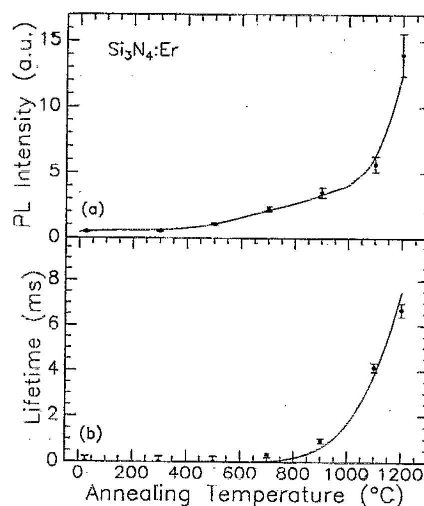

FIG. 9. (a) Room-temperature PL peak intensity and (b) fluorescence lifetime for implanted Si_3N_4 films measured at $\lambda = 1.535\ \mu$m as a function of annealing temperature. Annealing was performed in vacuum for 1 h. The lines are a guide for the eye.

Downloaded 15 Sep 2003 to 131.215.237.184. Redistribution subject to AIP license or copyright, see http://ojps.aip.org/japo/japcr.jsp

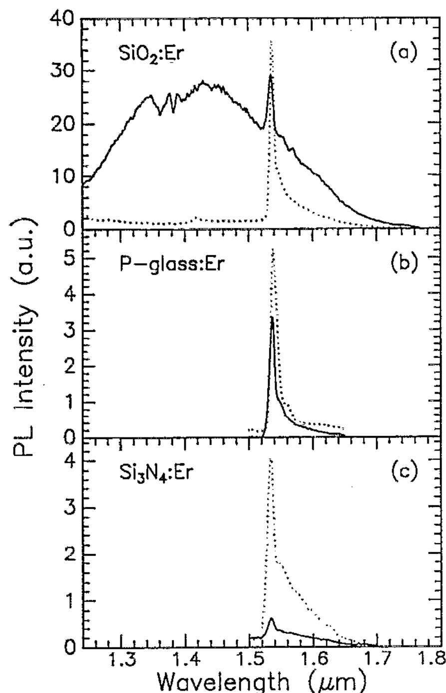

FIG. 10. PL spectra measured at 4.2 K for (a) as-implanted and annealed silica, (b) P glass and (c) Si_3N_4 films. Annealing temperatures are 1000 °C for silica and P glass and 1200 °C for Si_3N_4.

1200 °C. These measurements indicate that as-implanted Si_3N_4 is a highly defected material in which the optical transitions in the Er are quenched through their interaction with the host material.

4. Comparison between Er-implanted silica, P glass and Si_3N_4

a. Low-temperature PL. As the annealing characteristics of implanted silica, P glass and Si_3N_4 appear to be quite different, a more detailed study has been performed of the defect structure of these materials after implantation. Samples have been analyzed using PL spectroscopy at 4.2 K, and the results are shown in Fig. 10. PL spectra are shown for as-implanted (drawn lines) and annealed (dotted lines) films. Implantation conditions for each material were equal to those described in the previous sections. The annealing temperatures were 1000 °C for silica and P glass, and 1200 °C for Si_3N_4, respectively, and all anneals were performed for 1 h.

The spectrum for as-implanted silica shows a broad luminescence band which is attributed to implantation-induced defects in the silica network. This band is not observed in the room-temperature spectrum of Fig. 2. This indicates that the radiative transitions related to these defects are quenched at elevated temperatures. Superimposed on the defect band, the Er intra-4f transition at $\lambda = 1.535$ μm is observed. Figure 10(a) also shows that annealing at 1000 °C suffices to anneal out the defects as far as their optical activity at 4.2 K is concerned. A sharply peaked spectrum is observed in this case, with a tail extending to the high-wavelength region. This tail corresponds to the transitions from the lowest state in the multiplet of the first excited state to the ground state multiplet. Due to inhomogeneous broadening, no sharp peaks are observed. It should be noted that by using a single wavelength for excitation, only an isochromat of ions in the inhomogeneous distribution of sites is excited and the resulting fluorescence may not be representative of the entire ensemble of sites.

Figure 10(b) shows PL spectra for the implanted P glass films. No defect band is observed for the as-implanted sample, and thermal annealing only results in a slight increase in the PL intensity. These measurements clearly demonstrate the difference in network structure for as-implanted silica and P glass films. Indeed, these optical data show that optically active ions such as Er can be used as a probe of the local structure of a material. The observation of a broad defect-related luminescence band for implanted silica is consistent with the relatively low lifetime (6 ms) measured for the as-implanted sample (Fig. 3). The absence of this band for implanted P glass is reflected in the high lifetime (12 ms) for the as-implanted sample (Fig. 7). The difference between the behavior for silica and P glass might be explained by the softer network structure of the latter, which results in a more easy adjustment of the network to implantation damage. Also, it has been suggested[25] that *P*, when used as a codopant in rare-earth-doped silica glass forms a shell around the rare-earth ions which can enhance their solubility and cause a further decoupling from the silica network.

Data for Si_3N_4 are shown in Fig. 10(c) and are similar to those for P glass: a sharply peaked spectrum with a tail towards higher wavelengths is observed for both the as-implanted and annealed samples. The room-temperature PL measurements on Si_3N_4 indicate a significant amount of radiation damage in the as-implanted sample. The fact that no defect band is observed in the spectrum taken at 4.2 K indicates that these defects are of a different nature than those in silica; they do not exhibit optical transitions at 4.2 K.

b. Concentration quenching. Another way to investigate the local environment of the implanted Er ions is to investigate the concentration dependence of the optical properties. Samples have been implanted at fluences yielding Er peak concentrations in the range 0.1–2.0 at. %. Figure 11 shows the room-temperature fluorescence lifetimes measured at $\lambda = 1.535$ μm for all samples, as a function of Er peak concentration. Measurements are performed on samples annealed at 1000 °C (silica in vacuum, P glass in flowing N_2) or 1200 °C (Si_3N_4, in vacuum) for 1 h. For all three materials a decrease in lifetime is observed with increasing Er concentration. This suggests that for high Er concentration a nonradiative cross relaxation between Er ions takes place, leading to a spatial migration to quenching sites, resulting in a decrease of the fluorescence lifetime. These concentration quenching effects are an important finding from an application point of view. For instance, in a typical design of a planar Er-doped optical amplifier both high Er concentrations and long fluorescence lifetimes are required. The data from Fig. 11 can be used to determine the optimal tradeoff between concentration and lifetime.

Downloaded 15 Sep 2003 to 131.215.237.184. Redistribution subject to AIP license or copyright, see http://ojps.aip.org/japo/japcr.jsp

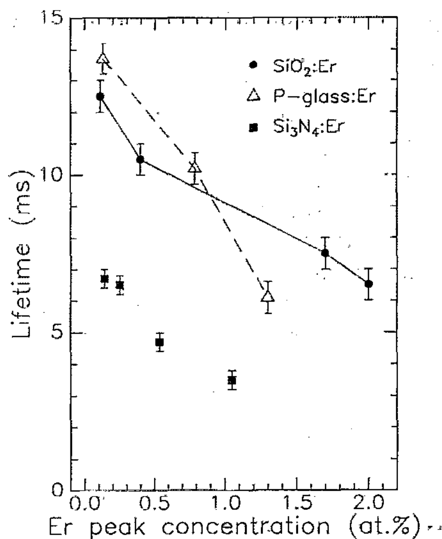

FIG. 11. Room-temperature fluorescence lifetime measured at $\lambda = 1.535$ μm for silica, P glass, and Si_3N_4 films as a function of Er peak concentration. Silica and P glass samples were annealed at 1000 °C, Si_3N_4 at 1200 °C. The lines are to guide the eye.

IV. CONCLUSION

This study shows that MeV ion implantation is a suitable technique to incorporate erbium on an optically active site in optical waveguide materials. After proper annealing treatment, Er-implanted silica, P glass and Si_3N_4 show a sharply peaked room-temperature luminescence spectrum centered around $\lambda = 1.54$ μm.

In the silica-based glasses, as-implanted samples show a relatively intense PL spectrum with a long fluorescence decay time (6 ms for silica, 12 ms for P glass). In the pure silica glass, thermal annealing at temperatures up to 1000 °C leads to an increase in PL intensity and lifetime, attributed to the annealing of beam-induced network defects. No measurable diffusion of Er occurs up to temperatures of 1200 °C (1 h). For an Er peak concentration of 0.1 at.% precipitation effects become dominant above 1100 °C. In P glass, beam-induced defects do not play an important role, and annealing does not further improve the fluorescence lifetime. This difference is interpreted in terms of the "softness" of the network structure of P glass which causes it to more easily accommodate implantation damage, and of the P forming a solvation shell around the Er, which decouples it from the network. Thermal annealing results in a change in the local configuration around the Er ions, and no diffusion of Er is detected for temperatures as high as 1000 °C (1 h). Defects play a more pronounced role in Er-implanted Si_3N_4. As-implanted samples show a very low room-temperature PL intensity and a lifetime below 0.2 ms. Thermal annealing at temperatures up to 1200 °C (and possibly higher) are required to anneal out the defects and obtain Er on an optically active site. No Er diffusion is detected at 1200 °C (1 h). Concentration quenching effects play a role in all implanted materials for Er concentrations in the order of 1 at. %.

Since Er implantation into all these materials results in intense and sharply peaked PL spectra with relatively long fluorescence lifetimes, the results of this study indicate that these materials can be used to produce Er-doped optical amplifiers, lasers and other integrated devices on a planar substrate.

ACKNOWLEDGMENTS

A. Lidgard and P. C. Becker are acknowledged for performing optical measurements in the initial stages of these experiments. We have greatly benefitted from discussion with G. W. Arnold, P. C. Becker, G. E. Blonder, A. J. Bruce, and C. H. Henry.

[1] A. M. Glass, Science **235**, 1003 (1987).

[2] C. H. Henry, G. E. Blonder, and R. F. Kazarinov, J. Lightwave Technol. **7**, 1530 (1989).

[3] H. J. Lee, C. H. Henry, K. J. Orlowsky, R. F. Kazarinov, and T. Y. Kometani, Appl. Opt. **27**, 4104 (1988).

[4] J. T. Boyd, Ed., *Integrated Optics: Devices and Applications* (IEEE, New York, 1990).

[5] P. Urquhart, IEE Proc. **135**, 385 (1988).

[6] L. Reekie, R. J. Mears, S. B. Poole, and D. N. Payne, J. Lightwave Technol. **LT-4**, 956 (1986).

[7] E. Desurvire, J. R. Simpson, and P. C. Becker, Opt. Lett. **12**, 888 (1987).

[8] R. J. Mears, L. Reekie, I. M. Jauncey, and D. N. Payne, Electron. Lett. **23**, 1026 (1987).

[9] S. Hüfner, *Optical Spectra of Transparent Rare-Earth Compounds* (Academic, New York, 1978).

[10] Y. Hibino, T. Kitagawa, M. Shimizu, F. Hanawa, and A. Sugita, IEEE Photon. Lett. **1**, 349 (1989).

[11] Our initial data on implantation doping of silica with Er are reported in: A. Polman, A. Lidgard, D. C. Jacobson, P. C. Becker, R. C. Kistler, G. E. Blonder, and J. M. Poate, Appl. Phys. Lett. **57**, 2859 (1990); A. Lidgard, A. Polman, D. C. Jacobson, G. E. Blonder, R. Kistler, J. M. Poate, and P. C. Becker, Electron. Lett. **27**, 993 (1991).

[12] P. D. Townsend, Nucl. Instrum. Methods B **46**, 18 (1990).

[13] P. J. Chandler, S. J. Field, D. C. Hanna, D. P. Shepherd, P. D. Townsend, A. C. Tropper, and L. Zhang, Electron. Lett. **25**, 986 (1989).

[14] Y. S. Tang, K. C. Heasman, W. P. Gillin, and B. J. Sealy, Appl. Phys. Lett. **55**, 432 (1989).

[15] D. Moutonnet, H. l'Haridon, P. N. Favennec, M. Salvi, M. Gauneau, F. Arnold d'Avitaya, and J. Chroboczek, Mater. Sci. Eng. B **4**, 75 (1989).

[16] J. Michel, J. L. Benton, R. F. Ferrante, D. C. Jacobson, D. J. Eaglesham, E. A. Fitzgerald, Y. -H. Xie, J. M. Poate, and L. C. Kimerling, J. Appl. Phys. **70**, 2672 (1991).

[17] H. Ennen, J. Schneider, G. Pomrenke, and A. Axmann, Appl. Phys. Lett. **43**, 943 (1983).

[18] G. S. Pomrenke, H. Ennen, and W. Haydl, J. Appl. Phys. **59**, 601 (1986).

[19] R. Brinkmann, C. Buchal, S. Mohr, W. Sohler, and H. Suche, Proc. Integr. Phot. Res. Conf., Hiltonhead, SC, USA, 26–28 March 1990.

[20] C. Shi, M. Tan, T. A. Tombrello, J. Non-Cryst. Solids **104**, 85 (1988).

[21] U. Katenkamp, H. Karge, and R. Prager, Radiat. Eff. **48**, 31 (1980).

[22] G. W. Arnold and P. Mazzoldi, in *Ion Beam Modification of Insulators*, edited by P. Mazzoldi and G. W. Arnold (Elsevier, Amsterdam, 1987).

[23] A. Polman, D. C. Jacobson, A. Lidgard, J. M. Poate, and G. W. Arnold, Nucl. Instrum. Methods B **59/60**, 1313 (1991).

[24] P. B. Klein and G. S. Pomrenke, Electron. Lett. **24**, 1502 (1988).

[25] K. Arai, H. Namikawa, K. Kumata, T. Honda, Y. Ishii, and T. Handa, J. Appl. Phys. **59**, 3430 (1986).

Downloaded 15 Sep 2003 to 131.215.237.184. Redistribution subject to AIP license or copyright, see http://ojps.aip.org/japo/japcr.jsp